ISSN-0366-6913

Cerâmica

ÓRGÃO OFICIAL DA ASSOCIAÇÃO BRASILEIRA DE CERÂMICA - ANO LIX- VOL. 59, 350 - ABR/MAI/JUN 2013

ASSOCIAÇÃO BRASILEIRA DE CERÂMICA

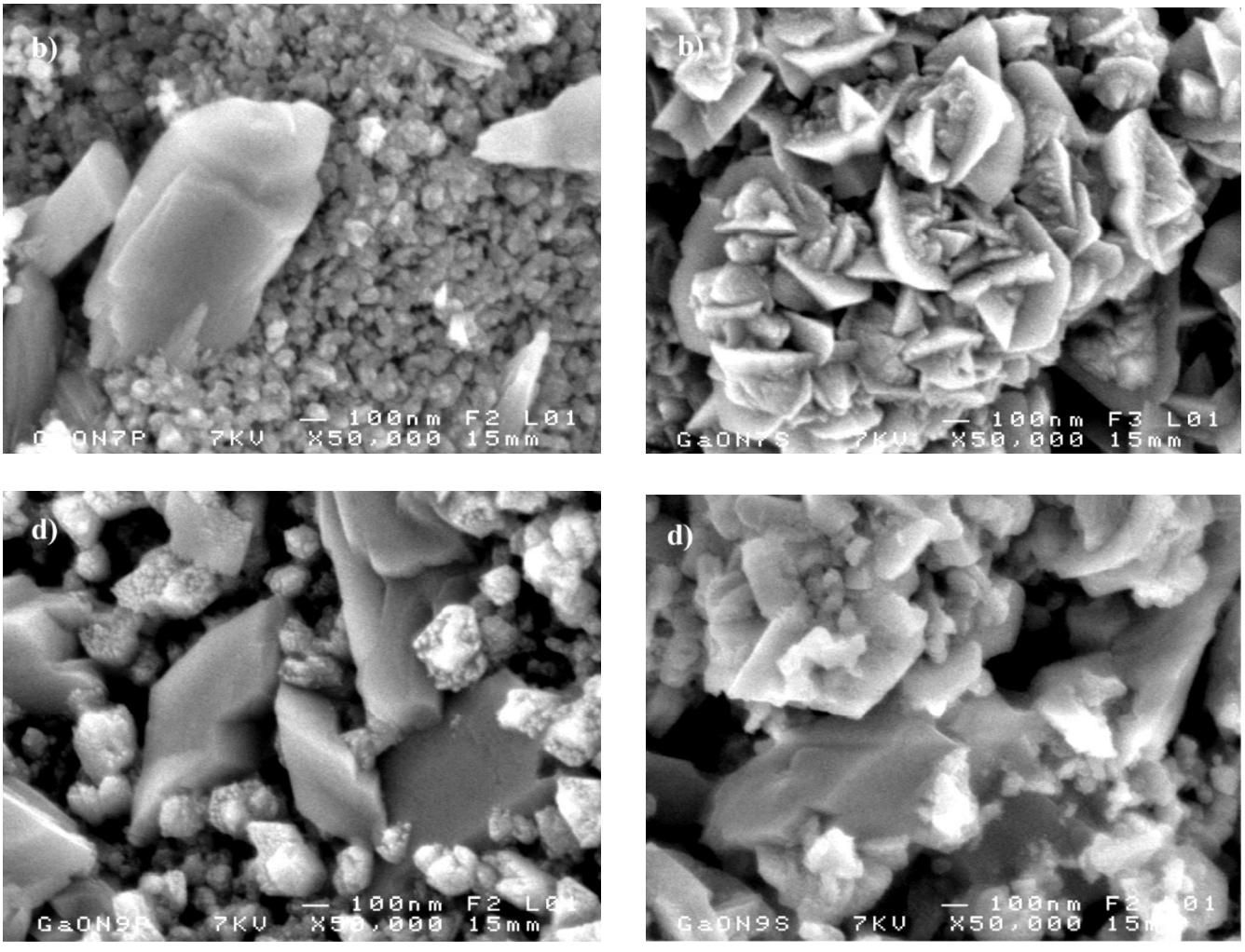

Zinc-gallium oxynitride powders: effect of the oxide precursor synthesis route

(Pós de oxinitreto de zinco e gálio: efeito da rota de síntese do óxido precursor)

J. F. D. Figueiredo[1,2], V. Bouquet[1], S. Députier[1], O. Merdrignac-Conanec[1], I. Peron[1], E. P. Marinho[4], A. G. Souza[3], I. M. G. Santos[3], M. Guilloux-Viry[1], I. T. Weber[2,5]

[1]Institut des Sciences Chimiques de Rennes, UMR 6226 CNRS/ Université de Rennes 1, Campus de Beaulieu, 35042 Rennes cedex, France

[2]LIMC, Departamento de Química Fundamental, Universidade Federal de Pernambuco, Recife, PE, Brazil 50740-560

[3]LACOM/INCTMN, Dept. de Química, Universidade Federal da Paraíba, Campus I, J. Pessoa, PB, Brazil 58059- 900

[4]Centro Acadêmico do Agreste, Universidade Federal de Pernambuco, Rodovia BR-104 km 59, Caruaru, PE, Brazil 55002-970

[5]Instituto de Química, Universidade de Brasília, Brasília, DF, Brazil 70910-900

ingrid@ufpe.br, itweber@unb.br

Abstract

Zinc-gallium oxynitride powders (ZnGaON) were synthesized by nitridation of $ZnGa_2O_4$ oxide precursor obtained by polymeric precursors (PP) and solid state reaction (SSR) methods and the influence of the synthesis route of $ZnGa_2O_4$ on the final compound ZnGaON was investigated. Crystalline single phase $ZnGa_2O_4$ was obtained at 1100 °C / 12 h by SSR and at 600 °C / 2 h by PP with different grain sizes and specific surface areas according to the synthesis route. After nitridation, ZnGaON oxynitrides with a GaN würtzite-type structure were obtained in both cases, however at lower temperatures for PP samples. The microstructure and the specific surface area were strongly dependent on the oxide synthesis method and on the nitridation temperature (42 m^2g^{-1} and 5 m^2g^{-1} for PP and SSR oxides treated at 700 °C, respectively). The composition analyses showed a strong loss of Zn for the PP samples, favored by the increase of ammonolysis temperature and by the higher specific surface area.

Keywords: nitride, oxide, chemical synthesis, surface properties.

Resumo

Oxinitreto de zinco e gálio foi sintetizado por meio da nitretação do $ZnGa_2O_4$ obtido pelo método dos precursores poliméricos (PP) e por reação no estado sólido (SSR). Foi estudada a influência do método de síntese do óxido precursor ($ZnGa_2O_4$) nas características do composto final ZnGaON. A cristalização do $ZnGa_2O_4$ foi observada após tratamento térmico a 1100 °C / 12 h para SSR e a 600 °C / 2 h para PP, sem a presença de fases secundárias em ambos os casos. Estas amostras mostraram diferenças no tamanho de cristalito e na área superficial em virtude do método de síntese empregado. Após a nitretação, em ambos os casos, foi obtida a fase oxinitreto ZnGaON com estrutura wurtzita, similar ao GaN. Entretanto esta fase se forma a temperaturas mais baixas quando PP é usado. A microestrutura e a área de superfície específica das amostras nitretadas foram fortemente influenciadas pelo método de síntese do precursor e pela temperatura de nitretação (42 m^2g^{-1} e 5 m^2g^{-1} para óxidos obtidos por PP e SSR e tratados a 700 °C, respectivamente). A análise da composição mostrou uma grande perda de Zn para as amostras derivadas de PP, a qual é favorecida tanto pela temperatura de amonólise quanto pela área de superfície específica do precursor.

***Palavras-chave**: oxiitretos, síntese química, propriedades de superfície.*

INTRODUCTION

Gallium oxide and nitride have been extensively studied due to their wide band-gap semiconducting properties, leading to various electronic and optoelectronic applications [1-4]. Less studied but also highly attractive is gallium oxynitride (hereafter called "GaON"), which has demonstrated a high potential for gas sensing and photocatalysis [5-7]. Improved or hybridized properties may also be obtained by doping "GaON" with different kinds of elements [8]. For instance, Li^+ doping is expected to change its gas sensing behavior and electrical properties [8] whereas Mn^{2+}-, Cr^{3+}-, and Fe^{3+}-doped gallium oxynitrides were studied to obtain a diluted magnetic semiconductor [9-11]. The doping of "GaON"

with In^{3+} and/or Zn^{2+} was also reported for water splitting under visible light irradiation [12-16].

Gallium oxynitride is described as an intermediate between GaN and Ga_2O_3 which typically crystallizes in a hexagonal (würtzite-type) structure [7, 14-16]. It is usually considered as a polytype of GaN. Moreover, it possesses some internal disorder and low crystallinity associated to oxygen content. Since both GaN and Ga_2O_3 are thermodynamically more stable than the oxynitride phase, the nitridation of Ga_2O_3 or the oxidation of GaN do not yield to an oxynitride under thermodynamic reaction control [10]. Experimental and theoretical investigations on the ternary system Ga-O-N confirmed that no crystalline or amorphous oxynitride phases appear during these reactions [17]. Synthesis of GaON was successfully obtained by nitridation under NH_3 flow of other gallium precursors such as $Ga(OH)_3$ [7, 12] or $NiGa_2O_4$ [5, 6]. Mn^{2+}- and Li^{+}- doped GaON were synthesized by nitridation of amorphous oxides obtained by the citrate route [8, 9].

Zinc gallium oxynitride (hereafter ZnGaON) presents high interest for visible-light photocatalytic activity [7, 14, 16, 18-20] but it may be very interesting also for gas sensing applications [5]. It is clearly observed that the choice of the starting materials affects the physicochemical properties. For these materials, mixtures of ZnO / Ga_2O_3 were used as starting material [14, 16, 21]. The use of amorphous oxide obtained by the citrate route [13] of crystalline $ZnGa_2O_4$ prepared by solid state reaction or of a mixture of $ZnGa_2O_4$ / ZnO [18] was also reported.

In this context, the influence of the synthesis route and thus of the physicochemical properties of $ZnGa_2O_4$ on the characteristics of the final compound ZnGaON was investigated in this present work. For the first time, $ZnGa_2O_4$ prepared by polymeric precursor method was used as nitridation precursor and compared to $ZnGa_2O_4$ prepared by the conventional solid state reaction.

EXPERIMENTAL

Synthesis of the $ZnGa_2O_4$ precursors

$ZnGa_2O_4$ powders were prepared by a conventional solid state reaction (SSR) from a mixture of appropriate amounts of ZnO (Alfa Aesar) and Ga_2O_3 (Strem Chemicals) heat treated in air between 800 °C and 1100 °C for 12 h. $ZnGa_2O_4$ powders were also synthesized by a polymeric precursor method (PP) based on the Pechini process [22] . In this present work, gallium nitrate (Strem chemical) and zinc acetate (Strem chemical) were added into an aqueous citric solution with a ratio [citric acid:cation] equal to [3:1] in mol. After the addition of ethylene glycol, with a ratio of [citric acid:ethylene glycol] equal to [60:40] in mass, the mixture was heated at 90 °C under continuous stirring and the obtained resin was submitted to two thermal treatments in air: (i) pre-treatment at 300 °C for 4 h to eliminate the organic matter (ii) annealing at 600 °C for 2 h to obtain the desired phase.

Nitridation of the oxide precursors

$ZnGa_2O_4$ powders obtained by both methods were nitrided in a tubular furnace under ammonia gas flow of 20 $L.h^{-1}$ for 24 h from 600 to 900 °C, with a heating rate of 10 °C.min^{-1} and cooling according to the inertia of the furnace. At 600 °C a 53 h longer NH_3 treatment was also experimented.

Characterization

Oxide and oxynitride powders were characterized by X-ray powder diffraction (XRD) (Philips PW 3710 diffractometer, Cukα radiation). The Ga/Zn ratio was obtained by energy dispersive spectroscopy (EDS) with a Jeol JSM 6400 scanning electron microscope equipped with an ISIS Oxford analyzer. The oxygen and nitrogen contents were determined by a LECO® TC-600 analyzer using the inert gas fusion method. The specific surface area was measured by the Brunauer–Emmett–Teller (BET) three point method using a Micromeritics FlowSorb II 2300 instrument. Before measurement, the samples were outgassed under N_2/ He flow at 250 °C during 30 min. The powder microstructure observations were carried out in a JSM 6310F field emission scanning electron microscope (FE-SEM).

RESULTS AND DISCUSSION

$ZnGa_2O_4$ precursors

Crystalline white $ZnGa_2O_4$ precursors were successfully obtained by the polymeric precursor method and conventional solid state reaction as evidenced by XRD (Fig. 1). In both cases, all reflections can be indexed according to a spinel-type structure (space group $Fd\bar{3}m$) with similar

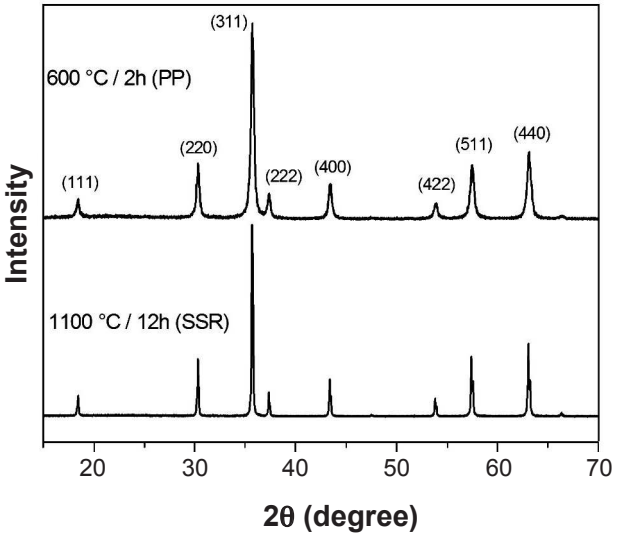

Figure 1: XRD patterns of $ZnGa_2O_4$ powders obtained by PP and SSR methods.
[Figura 1: Padrão de difração de raios X das amostras $ZnGa_2O_4$ obtidas pelos métodos PP e SSR.]

Table I - Lattice parameters (Å) and specific surface areas (m^2g^{-1}) of $ZnGa_2O_4$ obtained by PP and SSR routes.
[Tabela I - Parâmetros de rede (Å) e área superficial específica (m^2g^{-1}) do $ZnGa_2O_4$ obtido pelos métodos PP e SSR.]

$ZnGa_2O_4$	Lattice Parameters	Specific Surface Area (m^2g^{-1})
PP sample	8.33(4)	30
SSR sample	8.35(1)	<1

lattice parameters (Table I) and compatible with JCPDS file 38-1240 (a = 8.3349 Å). No peak assigned to other phase was observed. As expected, crystallization of the PP samples was much easier than the SSR ones (600 °C / 2 h and 1100 °C / 12 h, respectively). Indeed, a treatment below 1100 °C for the SSR route did not lead to crystalline $ZnGa_2O_4$ (not shown here). These results are in agreement with literature data. For instance, the synthesis of $ZnGa_2O_4$: Tb^{3+} by the Pechini method in the same temperature range was reported [23]. In this case, gallium was used as a precursor instead of gallium nitrate.

Fig. 2 shows the SEM micrographs of both samples. Different morphologies were obtained depending on the synthesis route. For SSR derived sample (Figs. 2c and 2d) agglomerates of different sizes (from hundred nanometers to several microns) were observed, whereas for PP one, porous aggregates were formed (Figs. 2a and 2b), comparable with literature data [23]. This different microstructure could be attributed to the release of CO_2 and H_2O during the decomposition of polymer network [23] and to the lower crystallization temperature of $ZnGa_2O_4$ in case of PP method. As a consequence, this precursor presented a higher specific surface area (30 m^2g^{-1}) than the one obtained for the oxide prepared by SSR (<1 m^2g^{-1}). Thus, the synthesis of $ZnGa_2O_4$ by two different routes yielded oxides with spinel structure but with different morphologies which will influence the nitridation process and the subsequent physico-chemical characteristics of the nitrided samples.

Zinc gallium oxynitride ZnGaON

The spinel phase transformed into a GaN würtzite-type structure (h-GaN) after ammonolysis at and above 700 °C

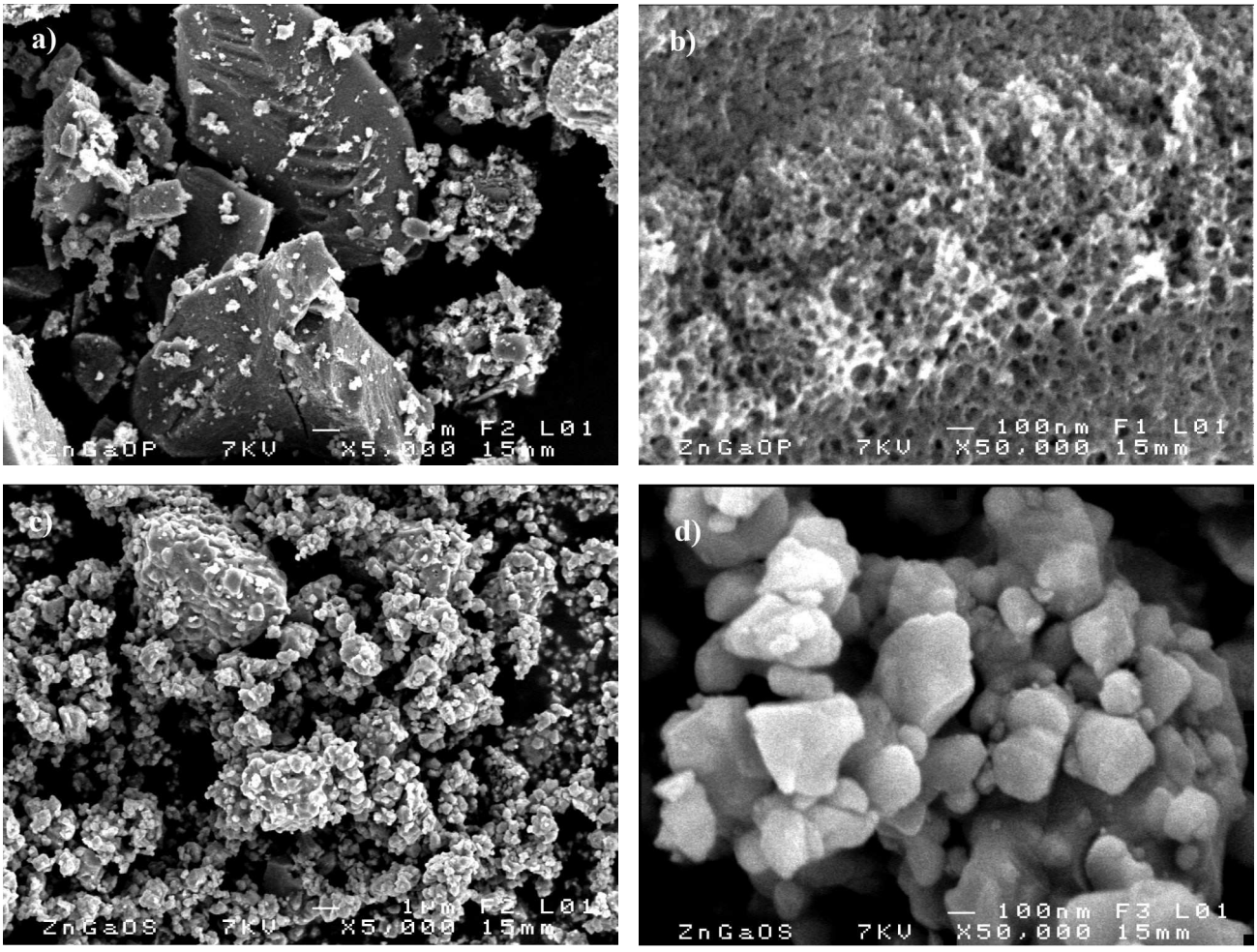

Figure 2: SEM micrographs of $ZnGa_2O_4$ prepared by (a,b) PP and (c,d) SSR routes.
[Figura 2: Micrografias obtidas em microscópio eletrônico de varredura das amostras de $ZnGa_2O_4$ preparadas pelos métodos (a,b) PP e (c,d) SSR.]

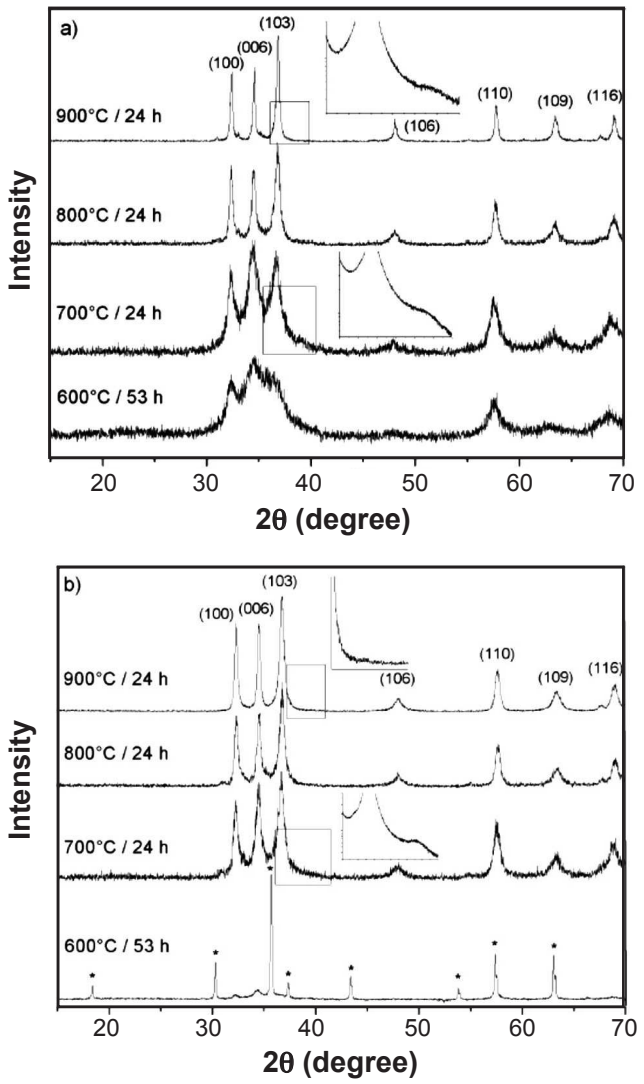

Figure 3: XRD patterns of the powders after nitridation at different temperatures of a) PP samples; b) SSR samples. Indexation was done according to $Ga_{0.97}N_{0.90}O_{0.09}$ JCPDS 32-0398 file. Peaks marked with * are related to $ZnGa_2O_4$.

*[Figura 3: Padrão de difração de raios X dos pós após a nitretação a diferentes temperaturas das amostras obtidas pelos métodos a) PP e b) SSR. A indexação foi feita de acordo com a fase $Ga_{0,97}N_{0,90}O_{0,09}$ do arquivo JCPDS 32-0398. Os picos indicados com * estão relacionados à fase $ZnGa_2O_4$.]*

for 24 h, whatever the oxide preparation method, without formation of any intermediate phase or amorphization. An increase of crystallization is observed at higher temperatures (Fig. 3). At 600 °C, the h-GaN was already obtained for PP derived sample but with poor crystalline quality whereas a mixture of the spinel oxide $ZnGa_2O_4$ with a few amount of würtzite was observed for SSR derived sample. In this last case, the provided thermal energy was not sufficient to totally transform the cubic structure of $ZnGa_2O_4$ into a h-GaN even for longer heat treatments (53 h). As expected, this result confirms that the morphology and specific surface area of the oxide precursor influence the nitridation threshold temperature.

The formation of ZnGaON from spinel $ZnGa_2O_4$ obtained by solid state reaction was described [21] as shown in equation A. In the present work, the porous morphology presented by PP derived samples favors the NH_3 diffusion improving the nitridation process.

$$\tfrac{1}{2}(1\text{-}x)\,ZnGa_2O_4 + 2/3\,(2\text{-}3x)\,NH_3 \rightarrow (Ga_{1-x}Zn_x)(N_{1-x}O_x) + (2\text{-}3x)\,H_2O + \tfrac{1}{2}(1\text{-}3x)\,Zn + 1/6\,(1\text{-}3x)\,N_2 \quad \text{with } x \leq 1/3 \qquad (A)$$

The XRD patterns obtained after nitridation at and above 700 °C are comparable to that of GaN, except for the presence of an additional low intensity peak around 40°, which can be observed for longer XRD acquisition routines (inserts of Fig. 3). The presence of this weak peak (generally associated with two other peaks at high angles, not shown here) suggests the existence of a polytype structure composed by a hexagonal and cubic closed-packed arrangement, which leads to an increase in unit cell parameters. The formation

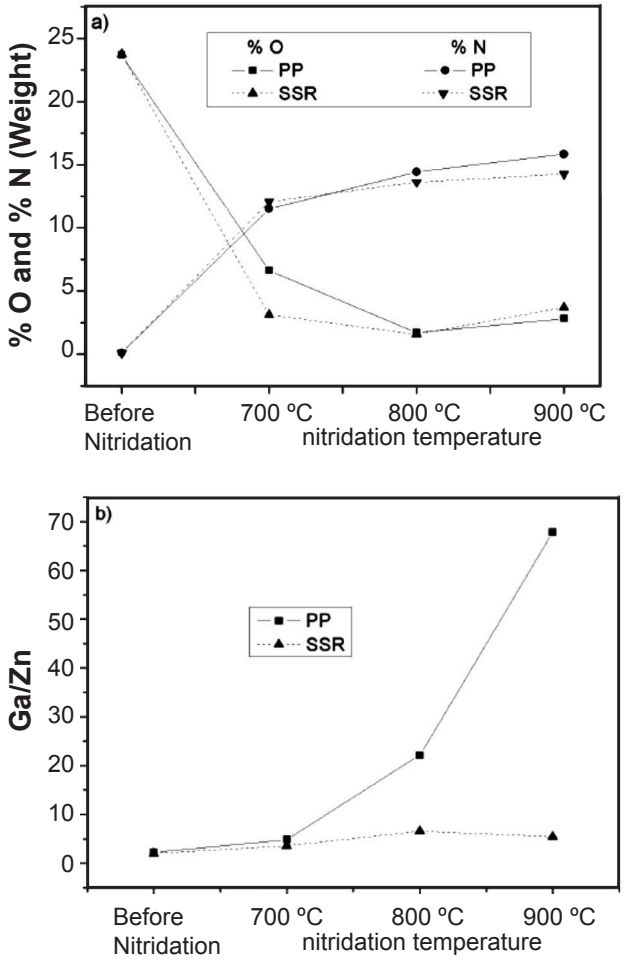

Figure 4: Composition analysis of PP and SSR samples before and after nitridation at different temperatures. a) oxygen and nitrogen content; b) Ga/Zn atomic ratio.

[Figura 4: Análise composicional das amostras obtidas pelos métodos PP e SSR antes e após a nitretação a diferentes temperaturas. a) Teor de oxigênio e nitrogênio; b) razão molar Ga/Zn.]

of this polytype in GaON derived from $NiGa_2O_4$ was already reported [5, 6] but it was not observed for ZnGaON obtained from $ZnGa_2O_4$ [19], amorphous precursors [13] or mixtures of ZnO / Ga_2O_3 [15]. Typically, the presence of these additional peaks is associated with a difference in the relative intensities of the three first diffraction peaks. However, in the present work the relative intensities are compatible with h-GaN structure, indicating the existence of a majority of hexagonal closed packing and a minority of cubic closed packing. For either, PP and SSR synthesis, the intensity of the additional peaks decreased when the nitridation temperature increased, indicating an evolution to the pure GaN hexagonal type-structure.

Considering these results and those reported [6], we have chosen to index all of the reflections with a hexagonal würtizte-type structure according to the JCPDS file 032-0398. This card is related to a gallium oxynitride compound with a space group $P6_3mc$ and $a = a_0 = 3.186$ Å and $c = 3c_0 = 15.530$ Å where a_0 and c_0 are the GaN parameters. The calculated lattice parameters obtained for the samples nitrided at 700 °C and 900 °C are summarized in Table II. For a nitridation at 700 °C, the *a*- and *-c* lattice parameters for the PP and SSR derived samples are larger than the values reported for GaON [6]. These results are attributed to the bigger Zn^{2+} (0.74 Å compared to 0.61 Å for Ga^{3+} [24]) present in our compounds, as shown by the estimated compositions (Table II) calculated from the chemical analysis. In both cases, the lattice parameters decrease with the increasing of the nitridation temperature because of the Zn^{2+} loss. Note that the same nitridation temperature, the PP derived samples present a smaller *a*-axis length and a bigger *c*-axis length than the SSR derived samples. This result could be attributed to the fact that the *a* lattice parameter is more sensitive to the Zn^{2+} content [16] whereas the substitution of O by N may occur along the c-axis [21].

The presence of incorporated nitrogen associated with the decrease of oxygen content was confirmed by composition analysis for the PP and SSR samples before and after nitridation (Fig. 4a). At 700 °C, the amount of incorporated nitrogen is 11.52 wt.%N (6.65 wt.%O) for PP derived sample and 12.07 wt.%N (3.14 wt.%O) for SSR derived sample. The increase of the nitridation temperature slightly influenced the nitrogen and oxygen contents for both samples, resulting in 15.84 wt.%N and 2.83 wt.% O for PP derived sample and 14.27 wt.% N and 3.72 wt.% O for SSR derived sample at 900 °C.

The EDS analysis (Fig. 4b) showed that before nitridation the Ga/Zn ratio was in agreement with the oxide formula using both SSR and PP methods. A Zn loss was observed after nitridation, favored by the increase of temperature. For PP derived samples, the Zn loss is much more pronounced and strongly dependent on the temperature: Ga/Zn = 4.84 and 67.81 at 700 °C and 900 °C, respectively (for SSR derived samples these values are 3.57 and 5.41, respectively). As a consequence, samples prepared by the PP method show a variety of compositions, which can leads to differences in photocatalytic activity or sensing behavior. During the $ZnGa_2O_4$ nitridation, spinel to würtzite phase transformation is correlated to the lengthening of the Zn-O bond which could lead to its breakage, favoring the loss of Zn. Thus, in PP samples this Zn-O elongation and breakage is favored [21].

The estimated compositions calculated from the chemical analysis of the samples nitrided at 700°C and 900°C are summarized in Table II. The PP derived samples clearly contain a small amount of cation vacancies, similarly to some literature data which use the citrate route [8-10, 13]. These vacancies are usually not observed for gallium oxynitrides prepared by nitridation of precursors obtained by solid state reaction [15, 18].

Figs. 5 and 6 show SEM micrographs of ZnGaON obtained from $ZnGa_2O_4$ prepared by PP and SSR routes and nitrided at 700 °C and 900 °C, respectively. For PP derived samples the ammonolysis reaction increases the porosity of the large aggregates until their rupture providing smaller aggregates or even isolated particles (Fig. 5). At the same time, formation of plate-like particles occurs. For SSR derived sample, agglomerates are still observed with a meaningful change in the particle morphology as round particles are substituted by plate-like ones after nitridation (comparison Figs. 2d and 6d). Increasing the nitridation temperature to 900 °C causes meaningful increase of the

Table II - Lattice parameters (Å), estimated compositions (calculated according to Refs. [8, 9] and specific surface area (m^2g^{-1}) of ZnGaON obtained by nitridation at different temperatures of PP and SSR samples. [Tabela II - *Parâmetros de rede (Å), composição estimada (calculada de acordo com [8, 9] e área de superfície específica (m^2g^{-1}) do ZnGaON obtido por meio da nitretação a diferentes temperaturas das amostras obtidas pelos métodos PP e SSR.]*

ZnGaON	a-lattice parameter	c-lattice parameter	Estimated composition	surface area (m^2g^{-1})
PP derived sample				
700 °C	3.19(6)	15.59(2)	$(Ga_{0.78}Zn_{0.16}\in_{0.06})(N_{0.66}O_{0.34})$	42
900 °C	3.18(8)	15.56(1)	$(Ga_{0.94}Zn_{0.01}\in_{0.04})(N_{0.86}O_{0.14})$	13
SSR derived sample				
700 °C	3.20(1)	15.55(5)	$(Ga_{0.79}Zn_{0.22})(N_{0.82}O_{0.18})$	5
900 °C	3.19(3)	15.54(1)	$(Ga_{0.84}Zn_{0.16})(N_{0.82}O_{0.18})$	9

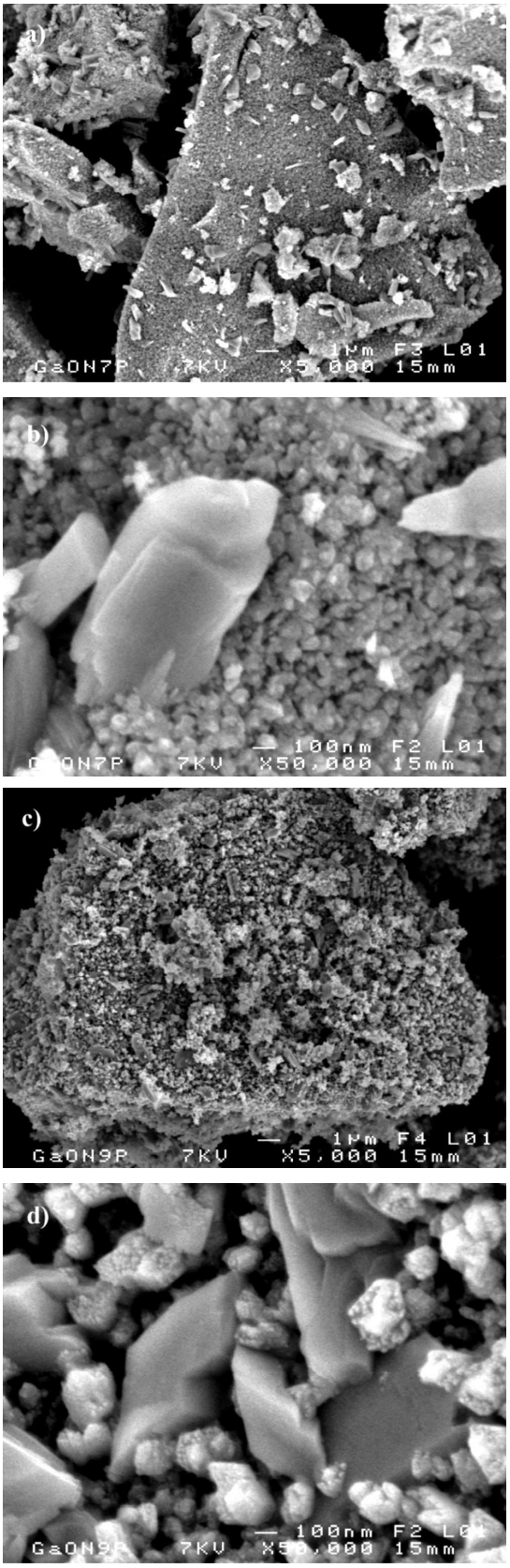

Figure 5: SEM micrographs of ZnGaON of PP derived samples obtained after nitridation at 700 °C (a and b) and 900 °C (c and d).
[Figura 5: Micrografias obtidas em microscópio eletrônico de varredura das amostras de ZnGaON obtidas a partir das amostras produzidas por PP após nitretação a 700 °C (a e b) e 900 °C (c e d).]

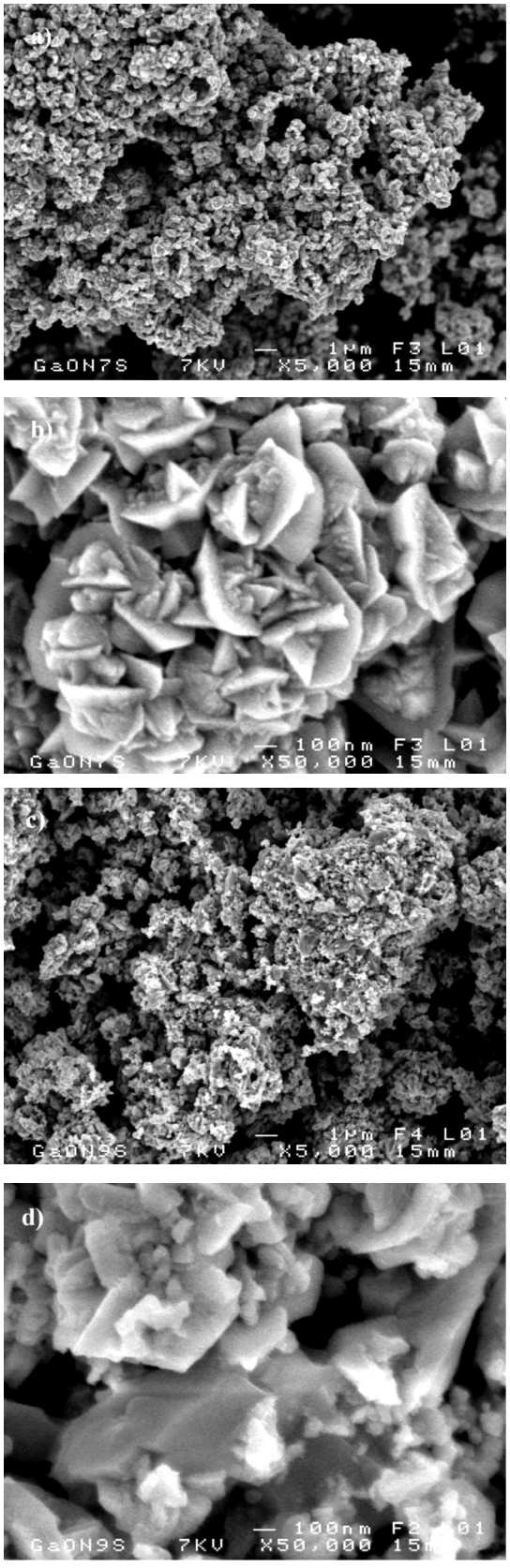

Figure 6: SEM micrographs of ZnGaON of SSR derived samples obtained after nitridation at 700 °C (a and b) and 900 °C (c and d).
[Figura 6: Micrografias obtidas em microscópio eletrônico de varredura das amostras de ZnGaON obtidas a partir das amostras produzidas por SSR após nitretação a 700 °C (a e b) e 900 °C (c e d).]

amount of plate-like particles due to the coarsening of the ZnGaON grains in the PP derived samples (Figs. 5c and 5d), making the microstructure resemble that of SSR derived powder (Figs. 6c and 6d).

Such a morphology with irregularly shaped particles was obtained after nitridation at 850 °C for 15 h of $ZnGa_2O_4$ prepared by conventional ceramic method [18]. The strong influence of the starting materials was observed in case of an initial mixture of ZnO / Ga_2O_3 [19]. In particular, the authors showed that the morphology of ZnGaON was strongly dependent of the initial morphology of ZnO but unaffected by the Ga_2O_3 polymorph. In the present work, we observed that the microstructure is sensitive to the precursor oxide morphology mainly for low nitridation temperatures and is almost not influenced for high nitridation temperatures. The nitridation strongly modifies the surface structure of the initial powders and consequently their specific surface area, as shown in Table II. For a nitridation at 700 °C, the surface area is strongly increased, mainly for the SSR derived samples. Nevertheless ZnGaON prepared from PP oxide presents a value 8 times higher (42 m^2g^{-1}) than the one obtained for the SSR derived sample (5 m^2g^{-1}). This high value decreases when nitridation occurs at 900 °C (13 m^2g^{-1}) and becomes closer to the value obtained for the SSR derived sample (9 m^2g^{-1}), in agreement with the SEM observations. A decrease of the surface area of GaON derived from $Ga(OH)_3$ with the increase of the nitridation temperature was also observed: 30 m^2g^{-1} and 12 m^2g^{-1} at 700 °C and 900 °C for 15 h, respectively [7]. The authors attributed this result to the coalescence of particles at high temperature. A surface area of 35 m^2g^{-1} for GaON after nitridation at 600 °C for 60 h of $NiGa_2O_4$ prepared by citrate route was observed [5] whereas values around 7 m^2g^{-1} were observed for ZnGaON prepared from a mixture of Ga_2O_3 and ZnO nitrided at 850 °C for 15 h [16].

From literature data and results obtained in this work, it clearly appears that a high specific surface area (important for photocatalysts and sensors) can be obtained providing that nitridation is performed at low temperature which is much easier when the precursors used are prepared by soft chemistry because they are more susceptible for the ammonolysis reaction, as a consequence of a porous morphology. Studies on the impact of these characteristics on their properties, in particular for gas sensor applications, are in progress.

CONCLUSIONS

Zinc gallium oxynitrides ZnGaON were successfully prepared from $ZnGa_2O_4$ synthesized by the polymeric precursor method (PP) and by solid state reaction (SSR). The use of two synthesis routes led to $ZnGa_2O_4$ with different morphologies which directly affected the diffusion of NH_3 and consequently the nitridation efficiency. The porosity of aggregates of the PP derived samples allows that the ammonolysis occurs throughout the sample, with spinel consumption at temperatures as low as 600 °C. Moreover, crystalline ZnGaON with high specific surface area was already obtained at 700 °C. Concerning particle morphology, PP and SSR derived samples presented very different morphologies when nitridation took place at 700 °C, however it became quite similar when higher temperature (900 °C) was employed.

ACKNOWLEDGEMENTS

The authors acknowledge CAPES-COFECUB (Project 644/09), FACEPE (Project APQ 0777-3.03/08), CNPq (Project 550388/2007-9), INCT/CNPq/MCT and PROINFRA/FINEP/MCT for financial support. F. Dagnone Figueiredo also thanks to FACEPE for a PhD grant.

REFERENCES

[1] S. Nakamura, M. Senoh, N. Iwasa, Shin-ichi Nagahama, Appl. Phys. Lett. **67**, 13 (1995) 1868.
[2] S. Nozaki, H. Feick, E. R. Weber, M. Micovic, C. Nguyen, App. Phys. Lett. **78**, 19 (2001) 2896.
[3] D-S. Lee, J-H. Lee, Y-H. Lee, D-D Lee, Sens. Actuators B **89** (2003) 305.
[4] M. Fleischer, H. Meixner, J. Appl. Phys. **74**, 1 (1993) 300
[5] M. Kerlau, O. Merdrignac-Conanec, P. Reichel, N. Bârsan, U. Weimar, Sens. Actuators B **115** (2006) 4.
[6] X. Cailleaux, M. d. C. Marco de Lucas, O. Merdrignac-Conanec, F. Tessier, K. Nagasaka, S. Kikkawa, J. Phys. D **42** (2009) 045408.
[7] C. C. Hu, H. Teng, J. Phys. Chem. C **114** (2010) 20100
[8] S. Kikkawa, K. Nagasaka, T. Takeda, M. Bailey, T. Sakurai, Y. Miyamoto, J. Solid State Chem. **180** (2007) 1984.
[9] S. Kikkawa, S. Ohtaki, T. Takeda, A. Yoshiasa, T. Sakurai, Y. Miyamoto, J. Alloys Compd. **450** (2008) 152.
[10] S. Yamamoto, S. Kikkawa, Y. Masubuchi, T. Takeda, H. Wolff, R. Dronskowski, A. Yoshiasa, Solid State Commun. **147** (2008) 41.
[11] S.Yamamoto , S. Kikkawa, Y. Masubuchi, T. Takeda, M. Okube, A. Yoshiasa, M. Lumey, R. Dronskowski, Mater. Res. Bull. **44** (2009) 1656.
[12] C-C. Hu, Y-L. Lee, H. Teng , J. Phys. Chem. Lett. **115** (2011) 2805.
[13] A. Miyaake, Y. Masubuchi, T. Takeda, S. Kikkawa , Mater. Res. Bull. **45** (2010) 505.
[14] K. Maeda, T. Takata, M. Hara, N. Saito, Y. Inoue, H. Kobayashi, K. Domen, J. Am. Chem. Soc. **127** (2005) 8286.
[15] M.Yashima, K. Maeda, K. Teramura, T. Takata, K. Domen, Chem. Phys. Lett. **416** (2005) 225.
[16] K. Maeda, K. Teramura, T. Takata, M. Hara, N. Saito, K. Toda, Y. Inoue, H. Kobayashi, K. Domen, J. Phys. Chem. B **109** (2005) 20504.
[17] M. Martin, R. Dronskowski, J. Janek, K-D Becker, D.Roehrens, J. Brendt, M. W. Lumey, L. Nagarajan, I. Valov, A. Borger, Progr. Solid State Chem. **37** (2009) 132.
[18] X. Sun, K. Maeda, ML Faucheur, K. Teramura, K. Domen, Appl. Catal. A **327** (2007) 114.

[19] T. Hisatomi, K. Maeda, D. Lu, K. Domen, Chem. Sus. Chem. **2** (2009) 336.
[20] K. Maeda, K. Domen, Chem. Mater. **22** (2010) 612.
[21] H. Chen, W. Wen , Q. Wang , J. C. Hanson, J. T. Muckerman, E. Fujita, A. I. Frenkel, J. A. Rodriguez, J. Phys. Chem. C **113** (2009) 3650.
[22] M. Pechini, US Patent 3330697 (1967).
[23] Z. Xu, Y. Li, Z. Liu, Z. Xiong, Mater. Sci. Eng. B **110** (2004) 302.
[24] R. D. Shannon, Acta Crystallogr., sect. **A32** (1976) 751.
(Rec. 03/10/2012, Ac. 03/11/2012)

Cerâmica

Ano LIX - Vol 59, 350, ABR/MAI/JUN 2013 - ISSN-0366-6913

CAPES

CNPq Conselho Nacional de Desenvolvimento Científico e Tecnológico

SciELO Brazil